JOURNAL OF GEOPHYSICAL RESEARCH VOL. 73, NO. 2 JANUARY 15, 1968

On the Generation, Dissipation, and Prediction of Ocean Wind Waves

T. P. BARNETT[1]

U. S. Naval Oceanographic Office, Washington, D. C. 20390

A method based on the equation of radiative transfer has been developed for predicting the two-dimensional wind wave spectrum in the North Atlantic Ocean. The model takes account of wave generation by both resonance and instability mechanisms. A simple representation for wave breaking is also included, as are the effects of nonlinear wave interactions. This combination of energy transfer mechanisms is used to compute wave spectra that are in reasonable accord with observations. The results question the concept of a 'fully developed' spectrum. The work also points up a lack of understanding of the particulars of various energy transfer mechanisms, as well as the shortcomings of the basic predictive input data.

1. INTRODUCTION

During the past ten years a number of theories have been presented to account for the growth and decay of wind-generated gravity waves. Unfortunately, there is very little data with which to confirm or dispute these theories. This increase in theoretical work has been matched by a definite need for more reliable open ocean wave predictions. It is the intent of this paper to combine these theoretical results and the results of recent experiments into a mathematical model that will lend itself to the evaluation of the individual theories and, at the same time, offer the basic framework for useful numerical wave prediction. That former goal will be accomplished by determining the quantitative theoretical forms that are required to produce successful hindcasts of wave energy spectra. The comparisons of these forms with those determined from theory make it possible to comment on the validity of individual theories. The latter objective, obtaining a useful wave prediction model, is implied by successfully computing waves under varied meteorological circumstances.

The reader is here warned not to expect to find the wave prediction problem solved in this paper. The emphasis is rather on establishing a framework for rational wave prediction. The details of the present scheme built within this framework will change greatly as our knowledge of wind waves increases. The results of the present paper help to point up both the practical and the theoretical areas where some of these changes must occur.

2. BACKGROUND

Recent advances in wave prediction. Significant progress has been made in the field of ocean wave prediction since the first efforts of *Sverdrup and Munk* [1947]. Substantial contributions have been made by *Pierson et al.* [1955], *Wilson* [1963], and others. The most important advances have come, however, from a group at New York University working under the direction of W. J. Pierson, Jr. [*Pierson et al.*, 1966] and a group in France headed by R. Gelci [*Fons*, 1966]. The interested reader is referred to these sources for any details.

Theory. Gelci et al. [1956], *Hasselmann* [1960], and *Groves and Melcer* [1961] have all independently proposed that the equation of radiative transfer provides an adequate description of wave propagation and the processes of generation and dissipation. This equation, which may be made to serve as a framework for wave prediction, reads

$$\frac{\partial F}{\partial t}(f, \theta, \mathbf{x}, t) = -\mathbf{V}(f, \theta)\cdot\nabla F(f, \theta, \mathbf{x}, t) + G(f, \theta, \mathbf{x}, t) \qquad (1)$$

where F is the two-dimensional energy spectrum and $\mathbf{V}$ is the group velocity of the component with true frequency f and geo-oriented direction

[1] Now at Westinghouse Ocean Research Laboratory, San Diego, California 92121.

Zubkovski, S. L., and T. K. Kravchenko, Direct measurements of some turbulence characteristics in the surface layer of the atmosphere over water, *Izv. Acad. Sci. USSR, Phys. Atmos. Oceans* (in Russian), *3*(2), 127, 1967.

Weiler, H. S., Direct measurements of stress and spectra of turbulence in the boundary layer over the sea, Ph. D. thesis, University of British Columbia, Vancouver, B.C., 1966.

(Received June 19, 1967;
revised September 14, 1967.)

θ measured clockwise from north. The spectrum F is defined so that

$$\iint F(f, \theta)\, df\, d\theta = \langle \zeta^2 \rangle$$

with ζ being the wave height. The first term on the right of equation 1 represents the propagation of wave energy and the second term, G, is a general representation of all processes that are adding energy to, or subtracting energy from, the spectrum. A formal derivation of (1) has been given by *Snyder* [1965]. We assume, as the boundary condition associated with (1), that there is no energy flow into the ocean from a coastline (no reflection). The initial conditions are $F(f,\theta,\mathbf{x},0)$, which, for the purposes of this work, will be taken as zero. If G were known and equation 1 could be integrated, it would be possible to predict waves with an accuracy that would depend only on the accuracy of the predicted wind field. A first attempt at incorporating recent concepts of wave generation and decay into G and solving the resulting equation are two goals of this paper.

It seems likely that a major part of the G function can be explained by the general theory of weak interactions recently suggested and developed by *Hasselmann* [1967]. The theory gives the rates of energy transfer for all expansible interactions between the wave field and the ocean-atmosphere fields. The wave generation theories of *Miles* [1957], *Phillips* [1957], and, presumably, *Phillips* [1966] are included in Hasselmann's theory. The general theory cannot, however, be quantitatively evaluated at the present time. In this paper, then, we consider a simplified G function. Two wave generation terms are used. They add energy to the spectrum in a linear [*Phillips*, 1957] and exponential [e.g., *Miles*, 1957; *Phillips*, 1966] manner. Wave dissipation within the generating region will be represented by wave breaking [*Phillips*, 1958]. The description of the G function is completed with the inclusion of wave-wave scattering processes, which may act in either a generative or a dissipative way. A more detailed description of G is deferred until section 3.

Recent observations of wave growth and dissipation. Until quite recently no reliable observations existed on the rate at which waves grow or decay. The first measurements of this kind have been made by *Snyder and Cox* [1966], *Snodgrass et al.* [1966], and *Barnett and Wilkerson* [1967]. The result of these three experiments will be of considerable importance later in this paper, and hence we review them here briefly.

In Snyder and Cox's experiment, a series of wave recorders was towed at a constant speed downwind from the lee of Eleuthera Island in the Bahamas. A singularity in the spectral transformation, relating the true frequency and direction of the wave to its apparent frequency and direction as observed by the moving recorders, allowed an estimate of the intensity of a single spectral component during its initial growth phases. This component had a group velocity that was equal to the towing velocity. Spectral growth curves were obtained for this single fixed-frequency component over a range of wind speeds. From these data it was possible to evaluate quantitatively the relative importance and correctness of the theories of wave growth previously mentioned.

In the swell attenuation study by *Snodgrass et al.* [1966], low-frequency spectral components were observed as they propagated along a great circle path across the Pacific Ocean from generating regions in the Antarctic and South Pacific oceans to the coast of Alaska. The study indicated that most attenuation takes place shortly after the waves leave the generating area. The authors concluded that this attenuation was not inconsistent with the energy transfer due to nonlinear wave interactions. After the primary attenuation, the components traveled over most of the Pacific Ocean (thousands of wavelengths) and exhibited no significant growth or decay, aside from that attributable to geometric spreading and island scattering. Neither following nor opposing winds seemed to have had any affect on the observed components.

In their limited-fetch study, *Barnett and Wilkerson* [1967] measured the rate of growth of the energy spectrum of ocean waves under steady wind conditions. Estimates of spectral growth were obtained from observations of steady-state, fetch-limited wave spectra that had been developed by an almost geophysically uniform wind field. The experiment was made after a strong low-pressure system had passed over the east coast of the United States and the steady offshore winds behind the frontal system

had established a stationary wave system in the area within several hundred nautical miles of the coast. An aircraft equipped with a high-resolution radar altimeter recorded continuous profiles of the sea surface from the coast to a distance of 190 nautical miles downwind from the coast. A similar run was made upwind. Considerable amounts of data were analyzed to show that the wind field was uniform in a geophysical sense.

Successive but independent sections of the measured sea surface profile along the direction of the wind were spectral analyzed to give the 'spectrum of encounter.' Care was taken to ascertain that the original data for each section met the condition of at least quasi-homogeneity. The true spectrum of each section was recovered on the basis of fundamental conceptions developed by *Cartwright* [1963]. The true spectra were insensitive to the assumed spectral spreading factor used in the recovery process. These data were then compared with various wave growth theories.

3. Specification of the G Function

The purpose of this section is to construct an expression for G (equation 1) that is jointly compatible with theory and experimental evidence and that will yield reasonable wave hindcasts. In early work it was thought that two generative terms, Phillips' and Miles', plus a wave breaking term based on an empirical representation for a 'fully developed' spectrum would be adequate to set up a working model with which to predict ocean waves. Under simple meteorological conditions, such hindcasts were of reasonably good quality. If the weather situation was complicated or the spectrum was changing rapidly, however, the results were poor. The failure, it turned out, was due in part to inadequate quantitative description of the generative terms and to the neglect of wave-wave interactions.

In the following specification of G, it has been sufficient to include four physical mechanisms that appear to have a first-order effect on the energy balance of the wave spectrum. Each of these mechanisms is treated separately, the goal being to make each agree with both theory and observation insofar as is possible. The individual mechanisms will be added to form the net function G, which then will be tested independently by hindcasts.

Evaluation of Phillips' resonance theory. The resonance theory of Phillips predicts that the energy of a particular spectral component grows linearly with time. The coefficient of this linear growth will be denoted by the parameter $\alpha = \alpha(f,\phi,\mathbf{x},t)$. It has been shown by *Hasselmann* [1960] that

$$\alpha = \frac{4\pi^2 k\sigma^3}{\rho_w^2 g^3} P(\mathbf{k}, \omega) \tag{2}$$

where $P(\mathbf{k},\omega)$ is the three-dimensional spectrum of the random atmospheric pressure fluctuations, $\sigma(= 2\pi f = (gk)^{1/2})$ is the circular frequency of gravity waves of wave number k, ρ_W is the density of sea water, and α has units of length squared per cycle.

From recent measurements by *Priestley* [1965] it has been possible to estimate P and hence α [*Snyder and Cox*, 1966; *Barnett*, 1966]. The measurements are consistent with the following form of P

$$P(\mathbf{k}, \omega) = \frac{\Phi(\omega)}{\pi^2} \left(\frac{\nu_2}{\nu_2^2 + k^2 \sin^2 \phi} \right) \cdot \left(\frac{\nu_1}{\nu_1^2 + (k \cos \phi - \Lambda)^2} \right) \tag{3}$$

The symbol ϕ indicates the angle between the wind (W) and wave directions. For $\phi = 0$, equation 3 reduces to the approximate relation (17) of *Snyder and Cox* [1966]. The other symbols are defined below.

1. $\Lambda = \omega/U$, U being the local 'convection velocity.' Priestley's data show that under conditions of atmospheric instability $U \simeq W$ several meters above the ground and for stable conditions $U \simeq W$ as measured at 0.2 wavelength above the mean surface. Λ has units of meters^{-1}.

2. ν_1 and ν_2 are empirically determined functions of Λ and are given by Priestley.

3. $\Phi(\omega) = \Omega(W, s, ?)\ \psi(\omega)$ and is the pressure power spectrum. ψ is apparently a universal function of ω. The data of Priestley show that it is given reasonably well, over the range of typical wind wave frequencies, by $1.23\ \omega^{-2}$. Ω is a turbulent scaling factor depending on the wind speed (W), atmospheric stability (s), and probably a number of other parameters. More will be said about Ω shortly.

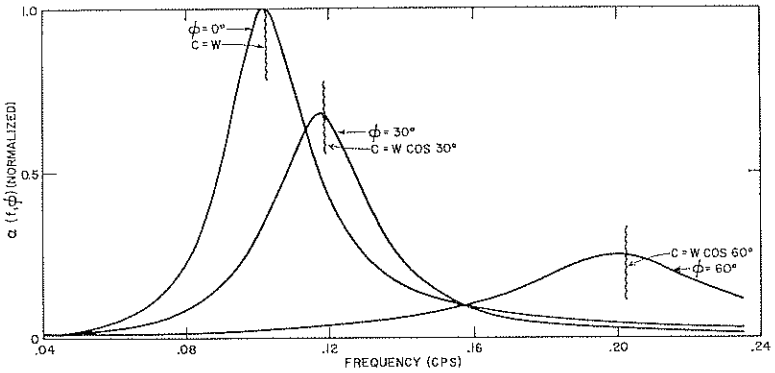

Fig. 1. Predictions of α (for $W = 30$ knots) from *Phillips'* [1957] theory, using estimates of the atmospheric pressure spectrum derived from the work of *Priestley* [1965]. ϕ is the angle between the wind and wave directions.

A plot of the resulting form of (2) for a typical wind speed of 30 knots (15.4 m/sec) is shown in Figure 1. The magnitude of α has been normalized pending a more detailed discussion of the turbulent scaling factor Ω. We note that α shows maxima at frequencies and angles that satisfy the 'resonance' condition, as predicted by Phillips.

To estimate the magnitude of α, it is necessary to arrive at a representation for Ω. Using the qualitative results of past experiments and Priestley's data, Snyder and Cox took Ω proportional to the fourth power of the mean wind speed. This form does not give a good comparison between (2) and measurements. Quite good agreement is obtained if Ω is taken proportional to the sixth power of the wind. This agreement is shown in Figures 2 and 3 for the Snyder and Cox experiment and the limited-fetch study. The comparisons are made more meaningful by the fact that the two sets of measurements each had a different geophysical variable (wind speed versus wave frequency). For the purpose of this paper we assume $\Omega \sim W^6$.

Representation for an exponential growth mechanism. Miles [1957] has considered the interaction between the wave field and the mean (laminar) atmospheric flow field. *Phillips* [1966] has considered the interaction between the wave field and undulatory turbulent flow due to the waves. Both these mechanisms give an exponential growth rate for the waves. The coefficient of this growth will be denoted by the parameter $\beta = \beta(f,\phi, \mathbf{x}, t)$. Limited data indicate that the theories are apparently not adequate to predict the observed exponential growth rate. Hence, the empirical form of β that we shall use should be regarded only as a working hypothesis.

Excellent information on β is provided by the measurements of Snyder and Cox. At least twenty-three estimates of the parameter were made for the ratios of wind speed to wave speed (W/c) between 1 and 2. A nondimensional plot of these estimates is shown in Figure 4. In the figure, the plus signs indicate lower spectral intensities (and presumably more accurate determination of β) and the squares indicate more advanced spectral development where nonlinear effects might be significant. Miles' theory is shown by the curve M, and the empirical relation

$$\beta = (\rho_a/\rho_w)(\mathbf{k}\cdot\mathbf{W} - 2\pi f) \qquad (4)$$

suggested by Synder and Cox is denoted SC. Here ρ_a is the density of air, and $\mathbf{W}$ is the wind velocity measured one wave length above the mean sea surface. Measurements of β made by Barnett and Wilkerson are also shown in Figure 4, the open circles and solid dots indicating data from the up- and downwind runs, respectively. For the downwind case, the agreement between the data and (4) is unexpectedly good. For the upwind case, there was practically no agreement. The disagreement between the up- and down-wind runs was explained by Barnett and Wilkerson as being due either to scattered, noisy data, and relatively poor curve fitting or to small changes in the near-shore wind field.

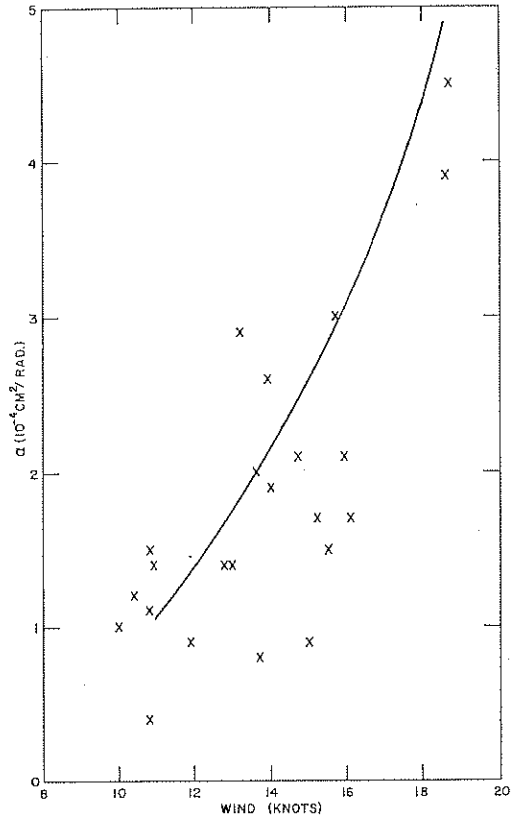

Fig. 2. Predicted values of α from section 3 (solid curve) compared with the measurements by *Snyder and Cox* [1966] (crosses).

On the basis of the above data, it will be assumed that a slightly modified form of (4)

$$\beta = \frac{5\rho_a f}{\rho_w}\left(\frac{W\cos\phi}{C} - 0.90\right) \qquad (5)$$

gives a reasonable estimate of β over a wide range of typical oceanic conditions. The modifications are prompted by the lack of knowledge of the wind profile over the ocean and by the fact that (5) gives a slightly better fit to the data. In the evaluation of (5), we take W as the wind measured at 19.5 meters above the sea surface (in accord with *Pierson et al.* [1966]). For $(W\cos\phi/C) < 0.90$, equation 5 represents a damping rather than a growth term. The measurements of *Snodgrass et al.* [1966] indicate that for long waves, at least, the damping is negligible. We shall accordingly assume $\beta = 0$ for $(W\cos\phi/C) < 0.90$. Both this assumption and the form of (5) will have to be

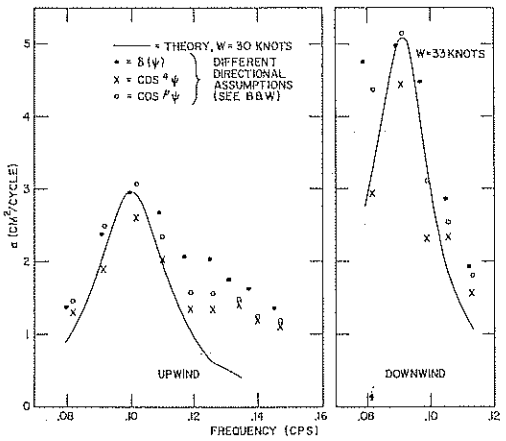

Fig. 3. Measurements of α from the limited-fetch study versus predictions of theory.

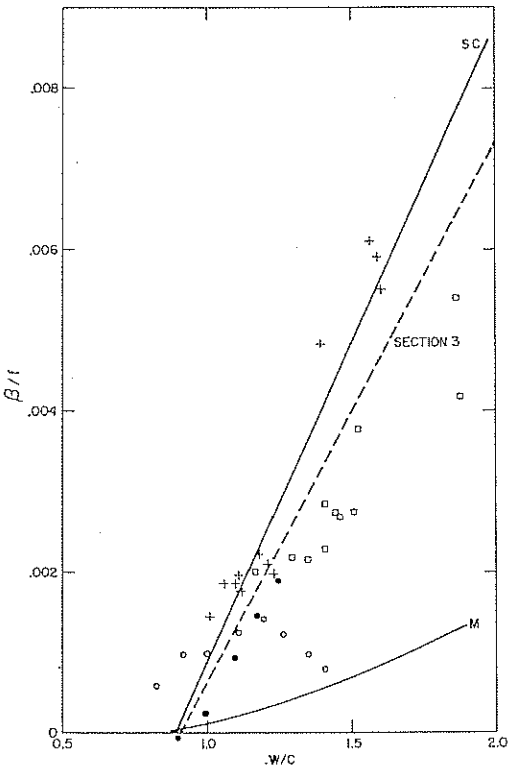

Fig. 4. Nondimensional plot of β versus wind speed. Data taken from *Snyder and Cox* [1966] (plus signs and squares) and *Barnett and Wilkerson* [1967] (open circles, upwind; solid dots, downwind). The curves marked SC and M represent the empirical suggestion of Snyder and Cox and the theory of *Miles* [1957], respectively. The dashed line is the form of β to be used in the prediction tests.

modified if the recent theories of *Phillips* [1966] and *Hasselmann* [1967] are verified.

Evaluation of the nonlinear wave-wave interaction theory. The evaluation of the wave-wave interactions involves cubic integrations. This requires several hours on a CDC 1604 computer [*Hasselmann*, 1963]. Clearly, this is incompatible with a practical wave prediction scheme. The purpose of this section, then, is to parameterize Hasselmann's results in a manner that will readily lend itself to rapid but accurate calculation.

The energy transfer due to wave-wave interactions is of the form

$$(\partial F/\partial t)_{nl} \approx \Gamma - \tau F \tag{6}$$

where Γ and τ are integral functions of F. To arrive at approximate expressions for Γ and τ, we characterize the wave field by the following parameters:

Energy

$$E = \iint F(f, \theta)\, df\, d\theta$$

Mean frequency

$$f_0 = \frac{1}{E} \iint F(f, \theta) f\, df\, d\theta$$

Mean direction

$$\theta_0 = \frac{1}{E} \iint F(f, \theta) \theta\, df\, d\theta$$

In terms of these parameters, good agreement with Hasselmann's computations were found by taking

$$\tau = \frac{7.5 \times 10^7 E^2}{g^4 f} \cdot (1 + 16\,|\cos(\theta - \theta_0)|) f_0^7 (f - 0.53 f_0)^3 \qquad f > 0.53\, f_0 \tag{7}$$

$$= 0 \quad \text{otherwise}$$

$$\Gamma = \frac{4.4 \times 10^8 E^3 f_0^8}{g^4} \cdot \cos^4(\theta - \theta_0) \left(\frac{f - 0.42 f_0}{f}\right)^3 \cdot \exp\left[-4\left(1 - \frac{f_0}{f}\right)^2 + 0.1\left(\frac{f_0}{f}\right)^5\right] \qquad f > 0.42 f_0 \quad \text{and} \quad |\theta - \theta_0| < \pi/2 \tag{8}$$

$$= 0 \text{ otherwise}$$

Equations 7 and 8 apply to spectra whose shape is not too dissimilar from a 'fully developed' spectrum. They also do reasonably well for a partly developed spectra, although the results would be enhanced by introduction of spectral shape factors. Estimates of τ from (7) are compared in Figure 5 with computations by Hasselmann for a Neumann spectrum with $\cos^4$ spreading factor. Figure 6 shows comparison of the rates of energy transfer as functions of wave frequency computed for a *Pierson and Moskowitz* [1964] spectrum [*Snodgrass et al.*, 1966]. With the above parameterizations, the computational time required to evaluate (6) was reduced to the order of a millisecond.

Representation for wave breaking. Within the wave-generating region and immediately beyond, the process of wave breaking (white capping) is of prime importance to the energy balance of the spectrum. Unfortunately, neither adequate observations nor a quantitative theory of wave breaking exists. *Phillips* [1958], using dimensional arguments, proposed that the func-

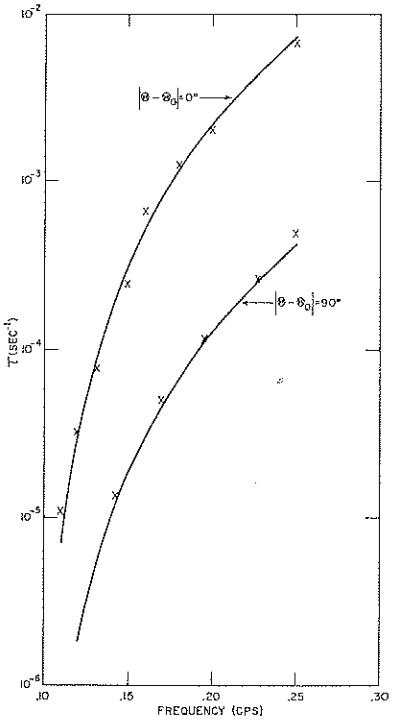

Fig. 5. Estimates of the reciprocal decay time from the theory of Hasselmann (crosses) and the parameterization equivalent from section 3 (solid lines).

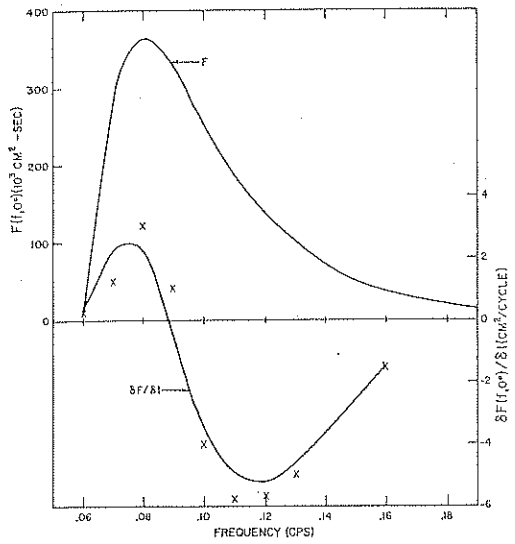

Fig. 6. The rates of nonlinear energy transfer for a typical 'fully developed' sea. Solid line denotes transfer rates from section 3, and crosses denote transfer rates from full theory [*Snodgrass et al.*, 1966, Figure 39].

tional form of the spectrum in the frequency range dominated by wave breaking, the 'equilibrium-range,' should be given by

$$R(f, \phi) = \frac{\gamma g^2}{(2\pi f)^5} H(\phi) \qquad (9)$$

where γ is a universal constant, H is an unknown angular spreading factor, and g is the acceleration of gravity. The quantity R is the limiting value that the (f_0, ϕ_0) component can attain. The f^{-5} power law has found a good deal of first-order experimental support [e.g., *Hidy*, 1965].

There is, however, a disturbing amount of variability in the exponent of f among various observers [e.g., *Kinsman*, 1960; *Burling*, 1959]. The limited-fetch study indicates that the process of wave breaking (or more generally, the energy balance of the higher-frequency parts of the spectrum) may be partly dependent on the location of the spectral peak, which would explain some of the scatter [*Barnett*, 1966].

For the present purpose, however, we will assume that an equation of the form (9) is an adequate first-order representation of the equilibrium range. Wave breaking will be taken into account by multiplying the wind generative terms α and β by the quantity $(1 - \mu)$, where

$$\mu = d_1 \exp\left[-d_2 \cdot (R - F)/F\right]$$

where d_1 and d_2 being constants. Data of *Longuet-Higgins et al.* [1963] as amended by D. E. Cartwright (personal communication), suggest that the angular spreading term in R might reasonably be taken proportional to $\cos^4 \phi$, with the accompanying normalizing factor. Since the wave-wave interaction effects are always negative in the wave-breaking region in the frequency range of interest, d_1 must be less than one in order to attain an equilibrium. The relative importance of the wave-wave effects in the breaking region is given by d_1, since for steady-state conditions

$$d_1 = 1 - [(\Gamma - \tau R)/(\alpha + \beta R)]$$

The limited-fetch data indicate that d_1 is in the range 0.7 to 0.8 for $\phi = 0$. The 0.8 value was used in the prediction tests. The exponential form of μ was chosen to achieve a sudden transition to equilibrium. The 'suddenness' is determined by d_2. In practice, d_2 is limited by the size of time step used in the numerical integration of equation 1. More will be said about this and the computational manner in which wave breaking was handled in the next section. The value $d_2 = \frac{1}{2}$ was chosen to agree with the limited-fetch data and the numerical requirements.

4. Numerical Solution of Radiative Transfer Equation

Numerical method. Adding all processes discussed above, we obtain the energy balance equation

$$\frac{\partial F}{\partial t} = -\mathbf{V} \cdot \nabla F + (\alpha + \beta F)(1 - \mu) + \Gamma - \tau F \qquad (10)$$

A numerical solution of (10) by the method of characteristics did not appear feasible, since different characteristics are coupled through the nonlinear terms. The numerical methods developed for similar radiative transfer problems in astrophysics [*Chandrasekhar*, 1950] and neutron transport [*Fleck*, 1963] are generally not applicable. This is due again to the nonlinearity in G and also to the deterministic, rather than probablistic, nature of the problem. The numerical approach that was used to solve (10) was a finite difference method.

The full details of the numerical procedure are presented elsewhere [*Barnett*, 1966], and only a summary is given here. The basic difference scheme was centered in both time and space, although backward time differences were used in the G function. The computational stability of this scheme for homogeneous forms of (10) is well known. For the full form of (10), it was not possible to determine the stability analytically. Extensive computer tests showed, however, that the nonhomogeneous numerical model produced stable solutions to steady-state problems. This strongly implies stability for the general nonhomogeneous case. Since the difference scheme did not appreciably amplify or damp solutions, the numerical errors (due to truncation) showed as changes in the velocity at which wave energy was propagated. The larger the truncation error, the slower the energy appeared to travel. As shall be shown later, truncation errors can, under certain circumstances, be of considerable significance.

The difference formulation was programmed and run on CDC 3600 and 3800 digital computers. Each machine had a core storage of slightly less than 65,000 48-bit words. For the open-ocean test case described in section 5, the run time was about 2.5 min/time step or about 1 hour per simulated day. Although steps were taken to optimize the program (e.g., buffering tapes forward *and* backward), it is felt that the run time could still be cut by about 20–50%. The computer program was general enough, so that it could easily allow for changes in parameters, generating function, and geometries.

Grid systems. The spatial system chosen is almost identical with that used by *Baer* [1963] and *Pierson and Tick* [1965]. The grid was square with approximately two degrees of latitude (120 nautical miles) on a side when mapped on a 30–60 Lambert conformal projection. On such a projection, great circles are almost straight lines, and, hence, a wave moving in a constant direction on the grid system will approximately follow a great circle. The sphericity of the earth is important if a wave travels distances approaching one-quarter of the earth's circumference [*Groves and Melcer*, 1961]. In the test cases to be considered in section 5, the maximum propagation distance was one-eighth of an earth's circumference and the square grid system introduced negligible errors.

Slight modifications were made to the Baer grid. To conserve computer time, points were dropped in the lower latitudes, where no appreciable winds occurred during the test cases. Several points were added along the edges of the grid to render it more susceptible to finite difference techniques. Neither of these changes significantly affected the prediction tests. The resulting grid of 325 points is illustrated in Figure 7.

The choice of temporal coordinate system is equivalent to choosing the time step for the numerical integration of (10). A time step $\Delta t = 1$ hour was chosen. This selection resulted from a balance of considerations involving computational stability, computer time, and the fact that the wind field was given every 6 hours and every 120 nautical miles. To avoid computational instability for the relatively high frequencies, the spectrum was taken to be in local equilibrium above a cutoff frequency, f'. This frequency corresponded to the frequency of waves that require 6 hours (120 nautical miles) for full development. The limited-fetch data were useful in determining the f' function.

Adequate definition of the spectrum in $(f - \theta)$ space is particularly important for evaluation of the nonlinear parameters. This, coupled with the fact that the focus of section 5 will be on low-frequency waves generated by high winds, led to the choice of the following eighteen frequency components for open-ocean hindcasts:

f = 0.044, 0.050, 0.056, 0.061, 0.067,
0.072, 0.078, 0.083, 0.089, 0.094,
0.100, 0.106, 0.111, 0.122, 0.133,
0.144, 0.161, 0.173 cps

Spectral resolution for low wind speeds below 15–20 knots will be rather poor, but open-ocean knowledge of such relatively light winds is also rather poor. The directions θ were chosen in 30-degree increments ($\pm 15°$) relative to the spatial grid system. This is consistent with uncertainties in the reported wind direction [*Baer*, 1963].

5. Tests and Discussion

A Consistency Check

Before proceeding with a large-scale computational effort, the model was tried for the sim-

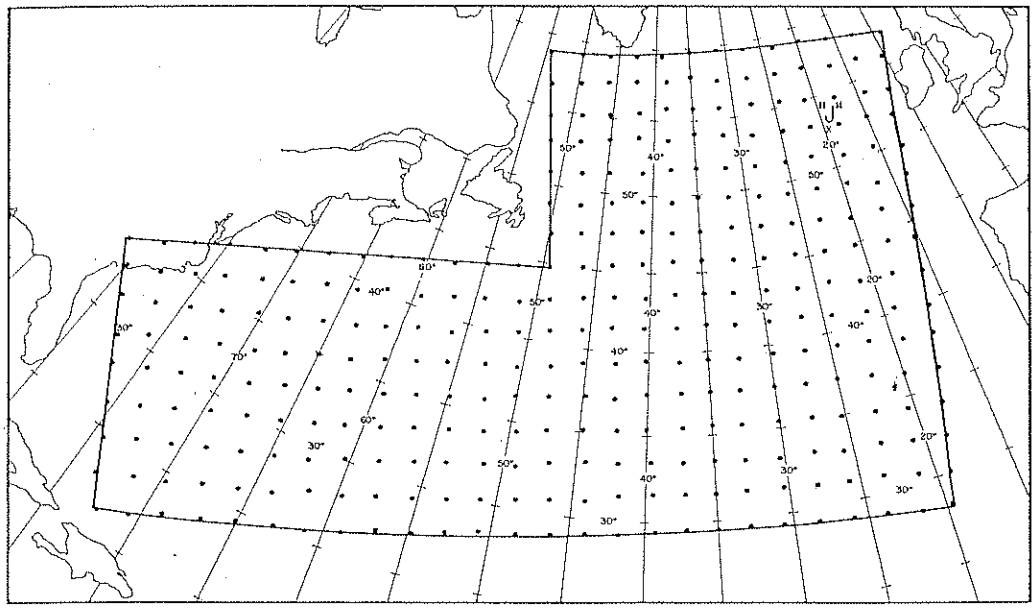

Fig. 7. The spatial grid system used to specify the wind and wave fields (test A). Polar stereographic, true at latitude at 60°. Grid is square on 30°–60° Lambert conformal map.

ple case of an infinite, uniform wind field. A steady 30-knot wind was assumed to start blowing abruptly over a calm ocean at time zero. After having blown for 30 hours, the wind ceased, and the spectrum was allowed to decay for another 30 hours.

The computed spectral growth is shown in Figure 8. Although the complete two-dimensional spectrum was calculated, only the one-dimensional spectrum is shown. It is seen that the major peak of the spectrum shifts rapidly toward the wind frequency $f_w (= g/2\pi W)$. After reaching f_w, it then shifts more slowly toward even lower frequencies. This is due primarily to the nonlinear interactions. The slight bump near $f = 0.09$ cps is due to the discontinuous 'cutoff' of the β mechanism. Although such a sharp cutoff is unrealistic, it will not significantly affect subsequent results.

This sequential development cannot be directly compared with measurement, but it can be compared against recent formulations for a 'fully developed' sea. The heavy dashed line of Figure 9 is the latest *Pierson and Moskowitz* [1964] spectrum. It is interesting and encouraging to note that the proposed model produces results that are in reasonably good agreement with the large amount of data embodied by the P-M spectrum. It is also apparent that, if the model is even reasonably correct, a stationary fully developed sea does not exist, since the nonlinear interactions constantly transfer energy toward lower frequencies. That extreme cases of this are not observed in nature is due to the abnormal durations and fetches that they would require. The fact that the spectrum is of constantly changing form may, however, be a contributing factor in the controversy over the proper empirical representations of the fully developed spectrum (see papers and discussions in *Ocean Wave Spectra,* Prentice-Hall, 1963).

After the wind ceases, immediate and substantial dissipation sets in, as illustrated in Figure 9. There are no measurements with which to compare the predictions, but the decay (as intended) is in qualitative agreement with the theory of Hasselmann (section 3) and the results of the swell attenuation study (section 2).

The Limited-Fetch Case

A more direct test of the model was offered by the observations of Barnett and Wilkerson for the classical case of a steady offshore wind. This comparison is not strictly independent, however, since some of the limited-fetch data were used in constructing μ and, to a lesser

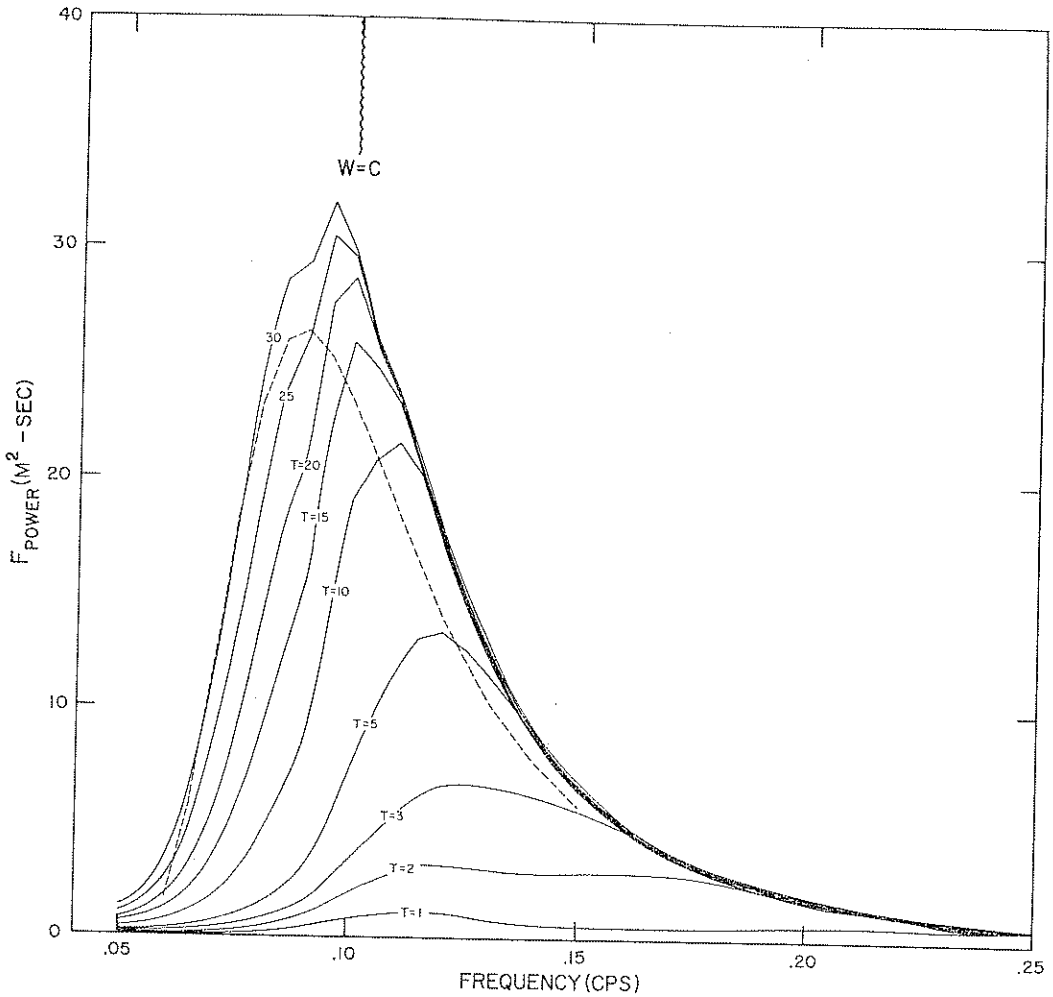

Fig. 8. Growth of the power spectrum starting from a calm sea over a 30-hour period. The fetch is infinite and the wind speed is 30 knots. The heavy dashed line is the latest *Pierson and Moskowitz* [1964] spectrum for a 30-knot wind. Solid lines, computed values from this study. Wind starts to blow at $T = 0$ hour.

extent, α and β. For the purposes of this test, the grid interval was reduced to 10 nautical miles and the time step to 20 minutes. The wind was taken at 32 knots, blowing directly offshore with a duration of 14 hours.

The resulting computed and observed growth curves for selected downwind components ($\phi = 0°$) of the two-dimensional spectrum are shown on Figure 10. The growth of the low- and mid-frequency components near the spectral peak is reproduced very well. For higher frequencies, both the distance required for equilibrium to be reached and the value of spectral density at equilibrium are given with reasonable accuracy. The intermediate parts of the observed growth curves are not reproduced well, however. This may be attributable to either: (1) the G function, as given in section 3, being incorrectly represented in this frequency region, or (2) the full growth of the higher-frequency components occurring in only a few grid intervals. Since the spectral energy is zero at the coast, this leads to large spatial truncation error. The grid interval is, thus, too gross to resolve the wave growth adequately in this case.

From previous tests and an evaluation of the truncation error, it appears that item 2 is a

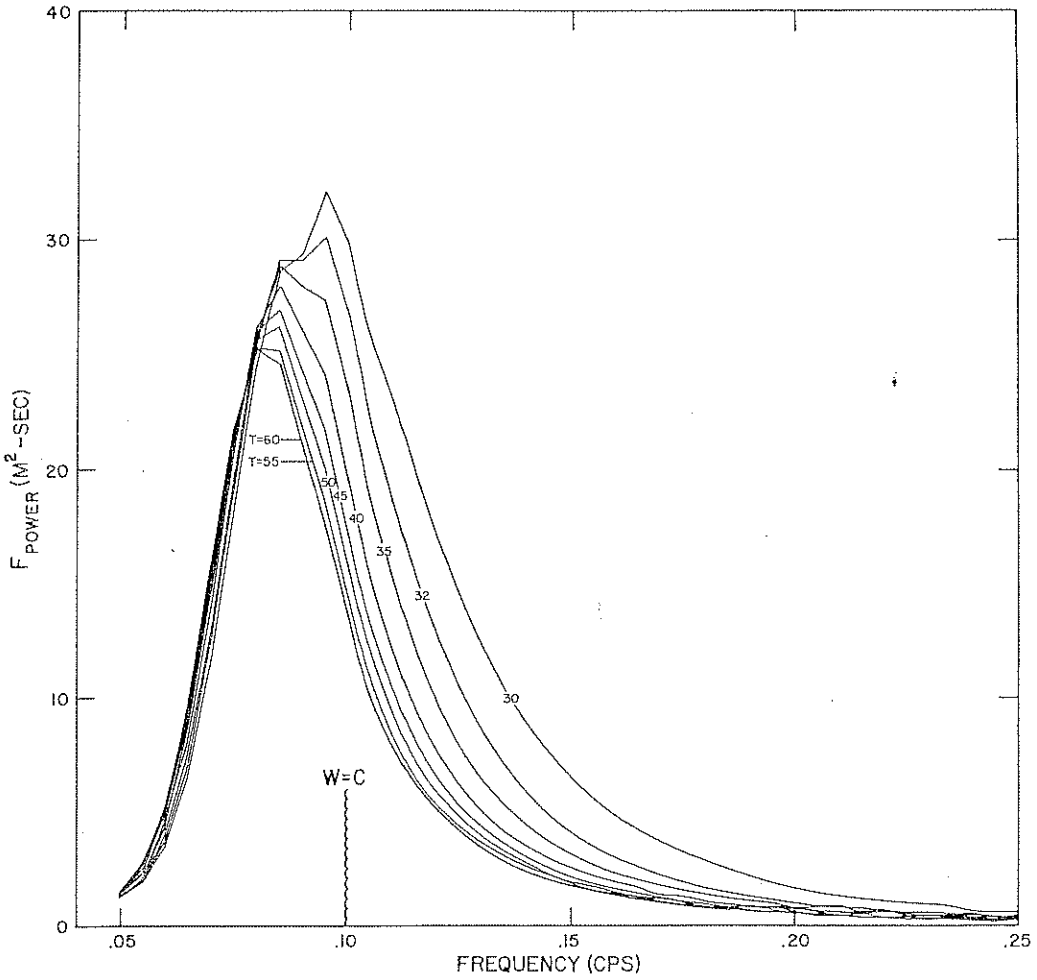

Fig. 9. Decay of the spectrum from time $T = 30$ hours, when the wind ceases, to time $T = 60$ hours.

major source of error. This indicates that the full system (120-nautical-mile grid) will not be reliable for the prediction of local waves near a lee coast. This unreliability could easily be remedied by a variable (finer) grid spacing near shore [e.g., *Bryan*, 1963]. For prediction in the open ocean, the problem is largely resolved by consideration of the high-frequency components at equilibrium with the local wind (section 4) and by the lack of a rigid boundary.

Although the limited-fetch test gives some confidence in the model, it cannot be construed as verification of the assumptions and suggestions made within this paper. This test together with section 3 does indicate, however, that the present model is compatible with most present theory and a wide range of geophysical data.

Open-Ocean Prediction Test

Background wave and wind data. In mid-December of 1959 a severe North Atlantic storm passed over the location of weather ship 'J' (near 52.5°N, 19°W, see Figure 7). The meteorological and oceanographic aspects of the storm are discussed in detail by *Bretschneider et al.* [1962]. The storm was accompanied by winds of 60 knots and significant wave heights of nearly 40 feet. After passage of the storm, the wave heights dropped from 36 to 14 feet in 12 hours. The storm offers an excellent but most

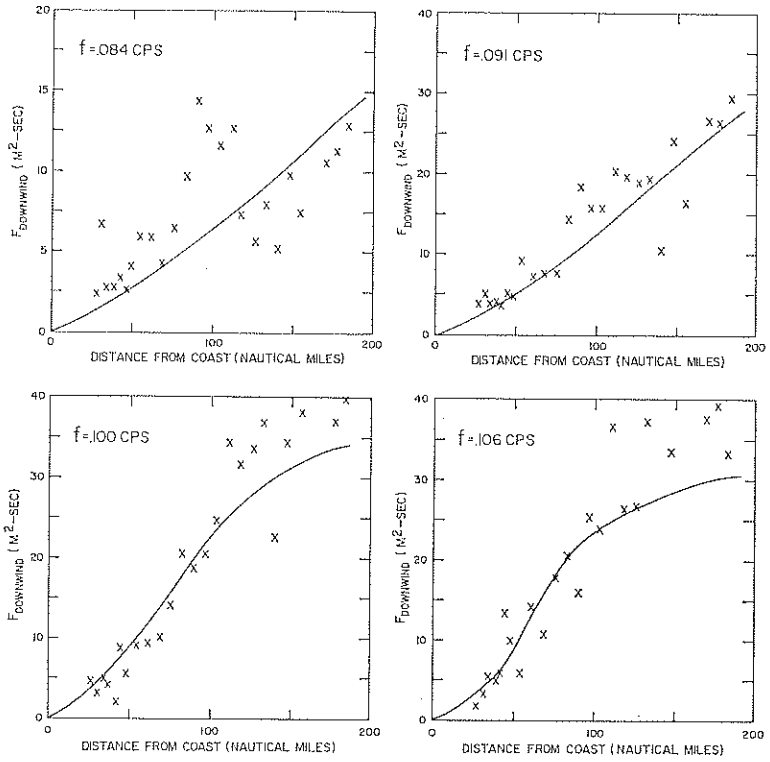

Fig. 10*a*.

difficult test to our model. This case also reveals most of the problems encountered in oceanic wave prediction.

Data: The observed wave spectra were obtained from analysis of wave records taken by the British weather ship *Weather Reporter*, as it *moved* out to occupy 'J.' The analysis is described in reports by *Moskowitz et al.* [1963] and by *Bretschneider et al.* [1962]. The 5 and 95% confidence limits on the observed spectra are variable but generally average 0.6 and 1.8, respectively. The wind field information was obtained in the manner described by *Thomasell and Welsh* [1963] and *Pierson and Tick* [1965] and was made available to the author through the generosity of W. J. Pierson, Jr.

Test conditions: Since the initial condition was taken to be a calm sea, the computations were begun about 4 days before the time that comparisons were to be made. This gave ample time for the effect of the initial conditions to die out. The test was conducted in two phases: Part A was run on the 120-nautical-mile grid shown in Figure 7; part B was run on an abbreviated grid with an interval of 60 nautical miles and was designed to provide information on the computational aspects of the problem. The grid points shown on Figure 7 below about latitude 43°N were excluded in part B because of lack of computer storage. This omission should introduce negligible errors, since the storm was above 45°N for most of its life and the observing ship was continually above 52°N. Reduction of the grid interval required (linear) interpolation of the wind field data for half of the grid points; errors so introduced are also small.

Results and discussions.

Significant wave height: The predicted and observed significant wave heights (H ⅓) are shown in Figure 11. The predicted values are taken from the grid point nearest the reported location of the ship. For the larger grid, two values are sometimes plotted.

The hindcasts of H ⅓ appear to be quite reasonable. That the results are smooth, as opposed to the (statistical) irregularity of the

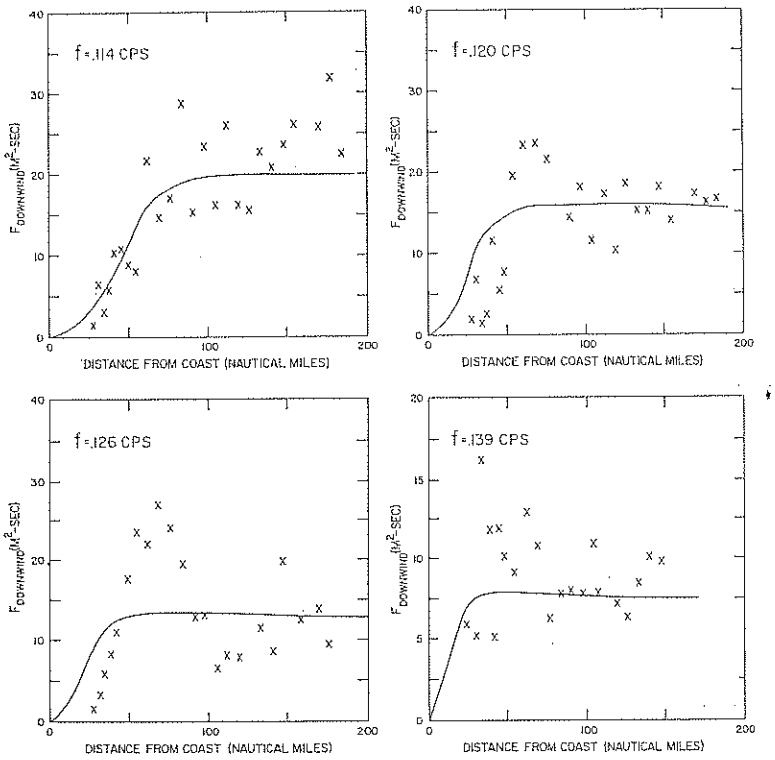

Fig. 10*b*.

Figure 10 shows the computed spatial growth curves for the case of a steady offshore wind similar to that encountered during the limited-fetch study. The crosses are observations from the limited-fetch study.

observations, is to be expected from both the manner in which the winds were determined and the computational method used. The wave heights appear to grow almost at the observed rate, but they do not drop as fast as the observed waves.

Part B consistently gives values that are lower than values for part A. The difference is apparently small, however, and there is no way to tell whether it arises from the computational procedure, better ship location on the grid, or slight differences in the wind field.

Spectral comparisons: Selected predicted spectra are shown versus observation in Figure 12. Only the one-dimensional spectra are plotted, since comparisons for the two-dimensional spectrum were not available.

We see that:

1. For the most part, the shape and magnitude of the predicted spectra are in reasonable agreement with observations.

2. The spectra peaks are well located. The actual spectral peaks are of slightly (one lag) higher frequency than the hindcasts, but the difference is not significant.

3. The f^{-6} law apparently allows too much energy in the frequency range 0.10–0.15 cps. This is construed as further evidence for the complexities (wind, exponent value, spectral coupling) involved in establishing and maintaining the equilibrium range.

4. Spectra *a*, *d*, *e*, and *f* (Figure 12) appear to be 'red-shifted' relative to observation.

This final point deserves special comment. For Figure 12*a* and 12*f* the ship was moving at approximately 5 knots when the data were taken. Since the ship was moving against the sea, one would expect the observed spectra (*a* and *f*) to be 'blue-shifted' relative to the real spectrum. The amount of frequency shift was estimated on the assumption that the ship was opposing a unidirectional sea. (The predicted

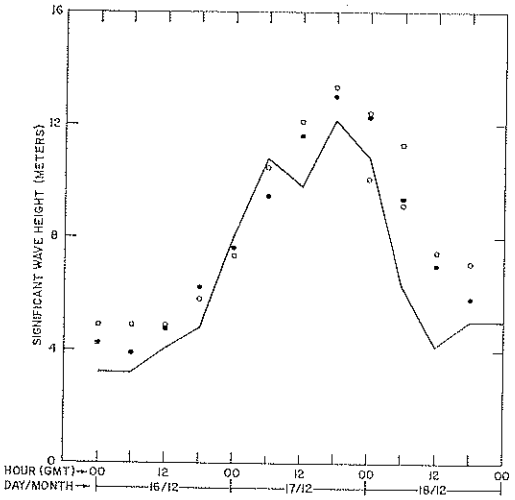

Fig. 11. Computed significant wave height for the reported position of the OWS *Weather Reporter* from 0000 UT December 16, 1959 to 0000 UT December 19, 1959. Open circles, computed values from 120-nautical-mile grid; solid dots, 60-nautical-mile, grid. For the larger grid, two values are sometimes plotted.

2-D spectra indicate that this is not a bad assumption for the lower-frequency waves.) Figure 13 shows both spectra after correction for ship motion. The agreement with the predicted spectra is considerably improved.

For spectra *d* and *e* (Figures 12*d* and 12*e*), the ship was moving 2 and 3 knots, respectively. In this case, the Doppler distortion is not sufficient to explain the discrepancies at the low frequencies and the steep forward face of the spectrum. Spectrum *d* exhibits considerable difference between tests A and B, but the same cannot be said for spectrum *e*. Hence, although some of the discrepancy is due to inadequate spatial resolution of a rapidly changing wave field, it also appears that these low frequencies are receiving too much energy. Since these waves are traveling somewhat faster than the wind, they are being generated mainly by the α mechanism. The most obvious deficiency in the representation for α is the turbulent scaling factor. More will be said about this later.

With specific reference to wave generation, the model generally performed well. Spectrum *b* is poorly predicted, but was generated during at least 3 hours of 60-knot wind (if the weather ship reports can be taken at face value) immediately behind the frontal system of the storm. The winds used for the hindcasts show 40–45 knots for this time. This explains spectrum *b* but also points out a failing of the wind program. If 'sharp' fronts and small areas of relatively high wind cannot be forecast, there is no way of determining the rapidly varying spatial and temporal features of the wave field.

The present scheme accounts reasonably well for the observed decay. It does seem to falter in spectrum *f*, however, and the discrepancy may be due to a number of causes:

1. The predicted winds are generally 10 knots higher during the decay period than observed by the weather ship.
2. Neglect of some unknown dissipative mechanism in G.
3. Generation of too much energy in the low frequencies initially.
4. Inherent smoothing of the finite difference approach.
5. Inaccurate ship location. Had the ship been 60 nautical miles (one grid interval) to the west of its reported location, the comparison would have been better.

All effects probably contribute to some degree. For the mid- and high-frequency range, cause 1 is of major significance, owing to the exponential nature of the proposed decay and to the fact that β and τ are essentially additive. For the lowest frequencies, the situation is different, since there is no effective way to dissipate the energy associated with these frequencies, once generated. The discrepancy in this frequency range may be explained by a combination of causes 3 and 4. The importance of cause 4 is illustrated by the marked difference between the results of test A and test B in Figure 12*f* (see also section 4).

The smaller grid interval gave more accurate comparisons than the larger interval did for the lowest frequencies, although no significant difference was found in the mid- and high-frequency range. The former result was to be expected from the rapid change of the wave field in both time and space. Taking the quality of present wind data into account, the method appears adequate for *present purposes* (i.e., everyday forecasting). The approach had shortcomings that could, however, be easily avoided in future work.

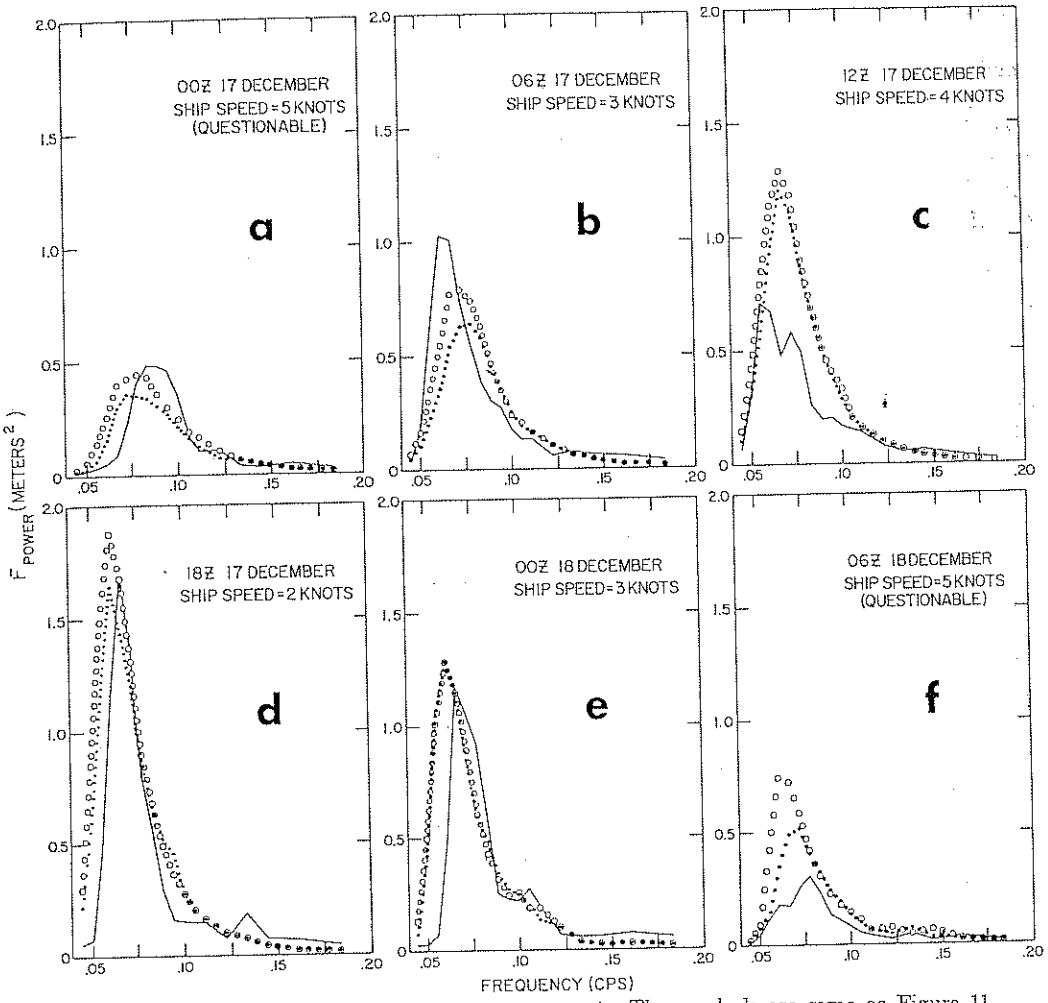

Fig. 12. Predicted power spectra versus measurements. The symbols are same as Figure 11. The speed of the ship at time of observation is also indicated.

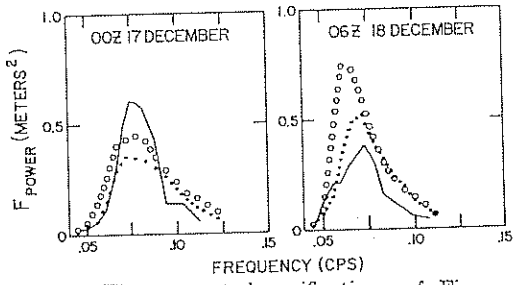

Fig. 13. The computed verifications of Figures 12*a* and 12*f* after correction for ship motion.

6. Summary

A method has been developed for predicting the two-dimensional wind wave spectrum in an area of the North Atlantic Ocean. This technique is as accurate as any proposed to date. The method utilizes the equation of radiative transfer and four energy transfer processes. Expressions for each mechanism were developed from available theoretical and experimental results. The reasonable success of the hindcasts indicates the importance of the four processes and, at the same time, raises some fundamental questions about wave growth, decay, and prediction.

The expressions for wave generation reproduce the observed wave growth rather well. Too much energy is predicted, however, at low frequencies, indicating that the form of α used is too large at high wind speeds. This may be

attributable to an inaccurate representation for the turbulent scaling factor Ω. On the other hand, it has been assumed that there are only two generation mechanisms. Recent work by *Hasselmann* [1967] indicates that α and β each represent the sum of two separate processes and that the generating functions are not independent of the wave spectrum, as has been assumed here.

The expression for wave dissipation is also uncertain. Although it appears that wave-wave interactions can account for a major part of the dissipation in some cases, there are still too many geophysical unknowns obscuring the picture to enable even a qualitative assessment of the general situation. Besides more extensive testing of prediction models, such as the one developed here, there is an immediate need for better measurements than now exist.

The accuracy of the general method is limited, at present, by the quality of available wind data. The grid size of the prediction scheme was adapted to the wind field resolution. The required spectral resolution is proportional to the propagation distance of the waves, i.e., the size of the prediction area. For the cases considered, the resolution chosen was adequate. The prediction of swell propagating over great distances, however, would require considerably higher resolution in both frequency and direction.

Acknowledgments. I am indebted to Professors R. Snyder and C. S. Cox and Dr. K. Bryan for informative and useful discussions during the course of this work. Special gratitude is due Professor Klaus Hasselmann for his assistance, encouragement, and suggestions as to the preparation of this manuscript. Professor W. J. Pierson, Jr., is also thanked for making available both wind field information and results of his recent work.

Messrs. J. J. Schule, Jr., and P. S. De Leonibus of the U.S. Naval Oceanographic Office and J. Barnett are acknowledged for providing the opportunity and climate required to carry out this work.

The majority of the work described herein was supported by the U.S. Naval Oceanographic Office. Additional support was provided by the Scripps Institution of Oceanography, the Institute of Geophysics and Planetary Physics at UCSD, and the Westinghouse Electric Corporation.

References

Baer, L., An experiment in numerical forecast of deep water ocean waves, *Lockheed Missile Space Co., LMSC-801296,* 1963.

Barnett, T. P., On the generation, dissipation, and prediction of ocean wind waves, Ph.D. dissertation, University of California, San Diego, 189 pp., 1966.

Barnett, T. P., and J. C. Wilkerson, On the generation of wind waves as inferred from airborne measurements of fetch-limited spectra, *J. Marine Res., 25*(3), 1967.

Bretschneider, C. L., H. L. Crutcher, J. Darbyshire, G. Neumann, W. J. Pierson, H. Walden, and B. W. Wilson, Data for high wave conditions observed by the O.W.S. 'Weather Reporter' in December, 1959, *Deut. Hydrograph. Z., 15*(6), 243, 1962.

Bryan, K., A numerical investigation of a nonlinear model of wind-driven ocean, *J. Atmospheric Sci. 20*(6), 594, 1963.

Burling, R. W., Wind generation of waves on water, Ph.D. dissertation, Imperial College, London, 181 pp., 1959.

Cartwright, D. E., The use of directional spectra in studying the output of a wave recorder on a moving ship, *Ocean Wave Spectra,* pp. 203–218, Prentice-Hall, Englewood Cliffs, N. J., 1963.

Chandrasekhar, S., *Radiative Transfer,* Oxford University Press, New York, 1950.

Fleck, J. A., Jr., The calculation of nonlinear radiation transport by a Monte Carlo method, in *Methods in Computational Physics,* vol. 1, edited by B. Alder, pp. 43–65, Academic Press, New York, 1963.

Fons, C., Provision de la houle, la méthode des densités spectro-angulaires 5, (D.S.A. 5), *Cahiers Oceanog., 18*(1), 15, 1966.

Gelci, R., J. Cazale, and R. Vassal, Utilisation des diagrammes de propagation à la provision énergétique de le houle, *Bull. Inform. Comité Central Oceanog. d'Étude Côtes, 8*(4), 169, 1956.

Groves, G. W., and J. Melcer, On the propagation of ocean waves on a sphere, *Geofis. Intern., 4*(1), 77, 1961.

Hasselmann, K., Grundgleichungen der Seegagsveroussage, *Schiffstechnik, 7,* 191, 1960.

Hasselmann, K., On the non-linear energy transfer in the gravity-wave spectrum, 1, General theory, *J. Fluid Mech., 12,* 481, 1962.

Hasselmann, K., On the non-linear energy transfer in the gravity-wave spectrum, 3, Evaluation of the energy flux and swell-sea interaction for a Neumann spectrum, *J. Fluid Mech., 15,* 385, 1963.

Hasselmann, K., Nonlinear interactions treated by the methods of theoretical physics (with application to the generation of waves by wind), *Proc. Roy. Soc. London, A, 299,* 77, 1967.

Hidy, G., The growth of wind waves on water in a channel, *NCAR Manuscript 66,* 18 pp., 1965.

Kinsman, B., Surface waves at short fetch and low wind speed—a field study, *Tech. Rept. 19, Chesapeake Bay Inst.,* 169 pp., The Johns Hopkins University, Baltimore, Md., 1960.

Longuett-Higgins, M. S., D. E. Cartwright, and N. D. Smith, Observations of the directional spectrum of sea waves using the motions of a

floating buoy, in *Ocean Wave Spectra,* pp. 111–132, Prentice-Hall, Englewood Cliffs, N. J., 1963.

Miles, J. W., On the generation of surface waves by shear flows, *J. Fluid Mech., 3,* 185, 1957.

Moskowitz, L. I., W. J. Pierson, and E. Mehr, Wave spectra estimated from wave recorders obtained by the OWS 'Weather Explorer' and 'Weather Reporter,' vol. 2, *New York Univ. Geophys. Sci. Lab. Rept. 63.5,* 1963.

Phillips, O. M., On the generation of waves by turbulent wind, *J. Fluid Mech., 2,* 417, 1957.

Phillips, O. M., The equilibrium range in the spectrum of wind-generated waves, *J. Fluid Mech., 4,* 426, 1958.

Phillips, O. M., *The Dynamics of the Upper Ocean,* pp. 1–261, Cambridge University Press, New York, 1966.

Pierson, W. J., G. Neumann, and R. James, Observing and forecasting ocean waves by means of wave spectra and statistics, *Hydrog. Office Publ. 603,* 180 pp., 1955.

Pierson, W. J., and L. I. Moskowitz, A proposed spectral form for fully developed wind seas based on the similarity theory of S. A. Kitaigorodskii, *J. Geophys. Res., 69*(24), 5181, 1964.

Pierson, W. J., and L. Tick, The accuracy and potential uses of computer based wave forecasts and hindcasts for the North Atlantic, *Proc. 2nd Military Oceanog. Symp.,* vol. 1, 69, 1965.

Pierson, W. J., L. Tick, and L. Baer, Computer based procedures for preparing global wave forecasts and wind field analyses capable of using wave data obtained by a spacecraft, *Proc. 6th Naval Hydrodynamics Symp.,* vol. 2, 1, 1966.

Priestly, J. T., Correlation studies of pressure fluctuations on the ground beneath a turbulent boundary layer, *Natl. Bur. Std. Rept. 8942,* 92 pp., 1965.

Snodgrass, F. E., G. W. Groves, K. F. Hasselmann, G. R. Miller, W. H. Munk, and W. H. Powers, Propagation of ocean swell across the Pacific, *Phil. Trans. Roy. Soc. London A., 259*(1103) 431, 1966.

Snyder, R. L., The wind generation of ocean waves, Ph.D. dissertation, University of California, San Diego, 1965.

Snyder, R. L., and C. S. Cox, A field study of the wind generation of ocean waves, *J. Marine Res., 24*(2), 1966.

Sverdrup, H. U., and W. H. Munk, Wind, sea and swell: Theory of relations for forecasting, *Hydrog. Office Publ. 601,* 44 pp., 1947.

Thomasell, A., and J. G. Welsh, Studies of the specification of surface winds over the ocean, *Travelers Res. Center Rept. 7049-88,* 44 pp., Hartford, Conn., 1963.

Wilson, B., Numerical Prediction of Ocean Waves in the North Atlantic for December, 1959, *NESCO Tech. Rept. SN-77-2,* 81 pp., 1963.

(Received May 25, 1967.)